AUTHOR	Juuso Suomi, Miika Meretoja
TITLE	Trends and irregular variation of spatial temperature differences in the high-latitude coastal city of Turku, Finland
YEAR	2021
DOI	https://doi.org/10.3354/cr01649
VERSION	Author's accepted manuscript
CITATION	Suomi J, Meretoja M (2021) Trends and irregular variation of spatial temperature differences in the high-latitude coastal city of Turku, Finland. Clim Res 84:41-57. https://doi.org/10.3354/cr01649

Trends and irregular variation of spatial temperature differences in the high-latitude coastal city of Turku, Finland

Juuso Suomi* and Miika Meretoja
Department of Geography and Geology, University of Turku, FI-20014, TURUN YLIOPISTO, Finland
*Corresponding author, e-mail: juuso.suomi@utu.fi

Abstract

Spatio-temporal dynamics of urban heat island (UHI) and other kind of spatial temperature variation was studied during the 17 year (2002-2018) period in the middle-sized (193 000 inhabitants in 2019) coastal city of Turku in south-western Finland. The study was based on geographic information systems (GIS) data and 30 minute interval air temperature observations in altogether 52 observation sites in the city and its surroundings. Correlation and regression analyses, image interpretation and various GIS methods were used to unravel the temperature dynamics and affecting factors on a diurnal, monthly and seasonal basis. The results showed relative cooling and warming trends of certain areas as well as fluctuating and random variation of coldest and warmest regions, respectively. Relative cooling trends were observed in semi-urban and urban areas that had kept unchangeable during the study period. Relative warming trends were most common in semi-urban areas where urbanization and construction of new buildings were fast and remarkable. Fluctuating variation was mainly related to the variation of weather conditions, especially to the severity of winter and related sea-ice extent on the archipelago to south-west of the city. The UHI intensity showed a statistically significant ($p \leq 0.01$) warming trend of 0.11 °C per decade. The findings of this study demonstrate the dynamic nature of spatio-temporal intra-urban temperature differences, the fact that should more actively be taken into account in climate related urban planning in general.

Keywords: climate change, land use change, local climate variability, sea ice cover, trend analysis, urban heat island

Running page head: 'Trends and irregular variation of temperature'

1. INTRODUCTION

Cities form specific type of local climate in their areas. Probably the most studied and also the most relevant manifestation of urban climate is urban heat island (UHI), which refers to the warmness of urban areas in relation to their rural surroundings. The principal thermo-physical factors behind the UHI include urban-rural differences in 1) solar heat storage and release, 2) anthropogenic heat release, and 3) evaporation. Solar radiation is stored as sensible heat in buildings and pavements during the daytime, promoted by good thermal conductivity and high heat capacity of typical urban construction materials. The stored heat is released in the air during the evening and night, resulting in a UHI as a consequence of slower cooling rate of the urban areas. Solar heat storage and release is the crucial reason for UHI in low latitudes throughout the year, and in middle and high latitudes in summer (Landsberg 1981, Oke 1987, Cotton & Pielke 1995). The most relevant sources of anthropogenic heat are traffic, industry and the heating/cooling of buildings. In high latitudes in winter, the role of anthropogenic heat release often exceeds that of solar impact in UHI formation (e.g. Klysik 1996). Due to the effective sewerage of storm water and impermeability of typical urban surface materials, the evaporation is often lower in urban areas, and a larger proportion of the heat is in sensible form thus promoting the formation of UHI (Cleugh & Oke 1986, Oke 1987, Cotton & Pielke 1995). Along with the fundamental thermo-physical factors described above, the UHI is also affected by city-specific features, such as city size, urban morphology, geographical location, topography and the nearby water bodies (Oke 1973, 1981, 1987, Wienert & Kuttler 2005). Consequently, also the UHI intensity and spatio-temporal characteristics of UHI vary from one city to the next.

UHI studies have earlier been focused on air temperature, i.e. canopy layer UHI (see e.g. Landsberg 1981, Oke 1987), and at simplest the UHI intensity has been defined as temperature difference

between an urban and a rural site (e.g. Emmanuel & Krüger 2012) or a set of urban and rural sites (e.g. Kolokotroni & Giridharan 2008). During last decades, the utilization of remote sensing in UHI studies has increased substantially, enabling studies on surface temperature differences, and consequently on surface urban heat island (SUHI) (Zhou et al. 2014, Estoque & Murayama 2017). Also the studies on interactions of UHI and SUHI have been conducted (Schwartz et al. 2012, Nichol et al. 2013). As UHI and SUHI are different urban climatic phenomena, also the connected study settings have their own case-specific benefits and bottlenecks. Air temperature and related canopy layer UHI directly reflect the thermal conditions that are relevant for a city dweller, whereas surface temperature can deviate much from the air temperature above, and as such is not in any case an optimal indicator of living conditions in the area. On the other hand, SUHI can often be investigated with a remote sensing data as a spatially continuous phenomenon, albeit in the limits of resolution, of course.

As canopy layer UHI is based on air temperature measurements that are often available only from specific locations, there is a challenge to get a comprehensive understanding of spatial temperature variation of a larger area. To tackle this challenge, point temperature data have been modelled to a spatially continuous surface with different interpolation and modelling techniques (Szymanowski & Kryza 2009, Hjort et al. 2016). Even if the air temperature has been recorded for a long time, the scarcity of observation sites has limited and still limits the possibilities to observe and study the spatio-temporal temperature variation in high resolution. With few observation sites, neither interpolation nor modelling methods quarantee reliable understanding on spatial temperature differences (Liu et al. 2017, Sillmann et al. 2017). Studies dealing with over a decade-scale change of canopy layer UHI have been earlier performed e.g. by Magee et al. (1999), Wilby (2003), Liu et al. (2007) and Levermore et al. (2018). In those studies, the UHI intensity has been in the focus, whereas the spatial pattern and especially the spatio-temporal change of UHI has been in a

negligible role, the fact probably being dictated largely by the sparsity of weather observation network with long-term observation history. In case of SUHI, the research frame have so far included also spatio-temporal change, but mostly over a 1-2 decade long period only (e.g. Zhang et al. 2013, Wang et al. 2016, Zhou et al. 2016, Yao et al. 2017).

Climate and climate change have been increasingly included in the urban planning globally, even if the city-specific differences in activity are still remarkable. The incorporation of local climate knowledge in urban planning, especially, varies a lot, resulting mainly from the scarcity of suitable data. If the cities are handled as a climatically homogenous units, a lot of relevant inputs for comprehensive urban planning will be lost. As in 2018, 55 % of the world' s population lived in cities, and the proportion is predicted to rise up to 68 % by 2050, climate change adaptation and mitigation related urban planning becomes even more important in the future (UN 2018). Even if information on local climate would be available, the evolvement of local climate in time remains a challenge. Once the local climate based city planning has been initiated, the plans should be controlled and updated regularly when needed (Grimmond et al. 2010). This study at hand aims to response to the above-mentioned challenges by producing novel information on spatio-temporal dynamics of temperature and relevant drivers behind in the middle-sized (193 000 inhabitants) high-latitude city of Turku. The study is based on temperature observations of an extensive local climate network during the 17 year period 2002-2018.

The detailed aims of the study are:

1) to find out, which kind of relative cooling or warming trends are detected in different parts of the study area
2) to find out, which kind of random variations are detected in the relative warmness / coldness of the different parts of the study area?

3) to find out, what are the seasonal characteristics of the observed trends and variations and which factors explain the observed variation?

2. MATERIALS AND METHODS

2.1 Temperature and environmental data

The temperature observations of Turku Urban Climate Research Group (TURCLIM) from a 17 year period (2002-2018) are used in investigating the spatio-temporal air temperature variation. The temperature data have been recorded at 30 minute interval with Hobo H8 Pro (2002-2010) and Hobo Pro U23-001 (2011-2018) loggers. The manufacturer-proclaimed accuracy of the instruments is ± 0.2 °C at 0-50 °C, while the resolution is 0.02 °C. Loggers are placed inside radiation shields on poles at three metres elevation, in order to minimise the risk of mischief in densely populated areas (Fig. 1).

Fig. 1 can be placed approximately here

The amount of sites with an uninterrupted observation period varies slightly on a monthly basis and on the temperature variable applied. Only the uninterrupted data series were included into the analyses resulting the amount of observation sites to vary between annual analyses' 24 and monthly analyses' 42. Altogether 52 observation sites were involved in the analyses of this study.

The changes in land use and land cover and their impact on temperature during the study period were estimated by comparing temporally separate versions of aerial photos (Turku 2020a), Corine Land Cover dataset (SYKE 2019) and SLICES land use classification (NLS 2010). The Digital Elevation Model (NLS 2000) was used to estimate the impact of topography on spatio-temporal temperature variation.

2.2 Statistical analyses

The spatio-temporal dynamics of temperatures was investigated by firstly setting the observation sites to the warmness orders for each case that was to be analysed. Thereafter, the changes in the warmness orders was investigated by fitting a linear trend to the time series or warmness order based ranks of the observation sites. The linear trend was fitted for monthly average temperatures, monthly averages of daily minimum temperatures and monthly averages of daily maximum temperatures. The daily minimum and daily maximum temperatures represent the coldest and warmest observation, respectively, during the 24 hour day defined to start at 0:00 local solar time (GMT+2). Random fluctuation in relative warmness without any detectable trend was studied by comparing the variation of monthly range lengths in the warmness order based ranks of the observation sites. To find out the connections between the weather and spatial temperature variability of the whole observation network, the standardized variation of warmness order based ranks were analysed together with the temperature anomalies from the average temperature of the month in question. With standardization the slight month-specific differences in the amount of observation sites available were taken into account.

The impact of unchangeable environmental factors on spatio-temporal temperature variation was estimated by calculating the Pearson's correlation coefficients between the observation sites':

a) month-specific range lengths in the warmness order based ranks and relative elevations
b) month-specific range lengths in the warmness order based ranks and proportions of water areas in the surroundings

The formulation of GIS-based variables was based on scale-specific testing and earlier experiences in the study area and in the other Finnish city, Lahti (Suomi et al. 2012, Suomi 2018). The impact of topography was assessed with relative elevation that was calculated by subtracting the elevation of

100, 200, 300 and 500 m radius buffers' average elevation around the logger site from the elevation of the logger site, resulting either in positive values (logger site is at the higher position than its surroundings) or in negative values (logger site is at the lower position than its surroundings). Relative elevation was preferred instead of absolute elevation as it has earlier proven to successfully reflect the climatic impact of topography in the study area (Suomi & Käyhkö 2012, Hjort et al. 2016, Väyrynen et al. 2017). The correlation coefficients with relative elevation and range length was calculated separately for each buffer size to sift the optimal buffer size. The proportions of water areas were calculated inside 500, 1000 and 2000 m radius buffers. Also the correlation coefficients with proportion of water areas and range length was calculated separately for each buffer size. The statistical analyses were performed with Microsoft Excel 2016 and IBM SPSS Statistics 25 and 26 software. The formulation of GIS-based variables was carried out with ArcMap 10.5.1 software.

The impacts of construction and other land use and land cover change were estimated with neighborhood and overlay analyses and visual comparison of the aerial photos and land use and land cover datasets representing different times during the study period 2002-2018.
The potential trend in UHI intensity was investigated by selecting one urban and one semi-urban observation site for UHI intensity calculations. The sites with rather unchangeable environment in their surroundings were selected in order the UHI intensity to better reflect the UHI pattern of the city as a whole, without too dominant impact of any large local changes. Also the effects of sea and topography were supposed to be rather similar between the selected two sites. The earlier experiences on spatial characteristics of UHI in the study area also affected the sites selection (Suomi & Käyhkö 2012, Hjort et al. 2016).

2.3 Study area

The study area consists of a middle-size (193 000 inhabitants in August 2019) coastal city of Turku and parts of its neighbouring municipalities. Turku (60°27'N, 22°16'E) is located in south-western Finland at the mouth of a river Aura that has an average discharge of 7 $m^3 s^{-1}$. The Baltic Sea coastline in the region is very irregular with an extensive archipelago of ca. 20,000 islands extending to the south-west of the city (Fig. 2). The total area of Turku is 306 km^2, of which the land areas cover 246 km^2. The shoreline length of the Turku municipality is approximately 200 km. The mainland areas of Turku are connected with bridges to the nearest islands Ruissalo (9 km^2) and Hirvensalo (12 km^2), located immediately off-shore the city centre. The nearest semi-open sea area Airisto is found approximately 10 kilometres to the south-west from the city centre (Suomi and Käyhkö 2012, Väyrynen et al. 2017, Turku 2020a). As a result, the climate of Turku is a combination of coastal and continental types, and depending on the movements of large weather systems, either one can dominate (Huovila 1987).

Fig. 2 can be placed approximately here

In Köppen's climate classification, Turku belongs to the Hemiboreal and humid continental *Dfb* class together with Baltic countries, southern parts of the Scandinavian Peninsula and majority of Eastern Europe. The same climate type also prevails in the Great Lakes region in the USA and at the mid-latitudes in the western part of Asia (Peel et al. 2007). The annual average temperature in the Turku airport, 7 km to the north of the city centre, is 5.5 °C (1981-2010). The coldest month is typically February, whereas July is the warmest, with average temperatures of -5.2 °C and 17.5 °C, respectively. The highest measured temperature in 1981-2010 was 32.1 °C (2010) and the coldest -34.8 °C (1987). Average annual precipitation is 723 mm, of which 30 % falls as snow. The duration of permanent snow cover is on average 90 days per winter, but annual variation is remarkable. Normally the snowy period starts at the end of December. The precipitation has seasonal variation

ranging from August's 80 mm to April's 32 mm. Cyclonic activity results in highly variable wind speed and wind direction. The average wind speed is 3.4 m s^{-1} and the dominant direction is SW with a 17 % proportion (Pirinen et al. 2012, FMI 2019).

The spatio-temporal extent of the seasonal sea ice cover is specific factor in the climate of Turku. The ice cover period typically lasts for three months, starting approximately at the end of the year. Depending on the seasonal weather conditions, the extent and timing may, however, vary notably between the years (Seinä & Peltola 1991, Seinä et al. 2006). For example, during the winters 2001-2020, the annual maximum ice cover proportion of the Baltic Sea varied between 9% and 79%, while the timing of the maximum ice extent stretched from 22nd of January to 24th of March (FMI 2020). Continuous sea ice effectively blocks the thermal effect of the sea, bringing about continental climate characteristic compared to ice-free conditions (Väyrynen et al. 2017).

The city centre of Turku consists of a grid plan area that has an extent of 4 km (SW-NE) times 1.5 km (SE-NW), and is approximately rectangular in form. The street network orientation follows that of a grid plan area, meaning that many of the streets are parallel to the dominant wind direction from SW. The market square in the middle of the grid plan is considered a core of the city centre. Blocks of flats and parks are the principal land use types in the grid plan area. The buildings are mostly 6-8 storey commercial and apartment buildings with varying surface colours and materials. The commercial areas are concentrated in the surroundings of the market square, whereas the rest of the built grid plan area consists of residential areas. The 50-100 metres wide river Aura flows through the city centre from the NE to the SW. Industrial areas (dock yard, heavy/light industry) and retail parks are mostly located outside the grid plan area on the western and northern side of the city centre. The rest of the land cover consists of forests, fields and mosaic of suburbs. The largest

sparsely populated areas are found towards the north of the city centre (Suomi & Käyhkö 2012, Hjort et al. 2016, SYKE 2019, Turku 2020a).

Topographically, the grid plan area consists of flat clay ground 5-10 meters above the sea level, on many sites broken through by 30-50 metres high bedrock outcrops. The largest parks on the grid plan area are located on the hills, and, consequently, they are only partially covered by buildings. Outside the grid plan, hills alternate with flat areas and the basic elevation rises gently inland. The highest places rise approximately 70 metres above the sea level (NLS 2000, Suomi et al. 2012).

4. RESULTS

4.1 Spatio-temporal temperature variation during the study period

The annual average temperature of 24 temperature loggers with uninterrupted observation period varied between 4.6 °C and 7.5 °C (Fig. 3). The average temperature of the observation period was 6.4 °C. The respective values for daily minimum temperatures were 0.8 °C, 4.1 °C and 2.8 °C, and for daily maximum temperatures 8.0 °C, 10.7 °C and 9.8 °C. During the 17-year study period the temperature trend was in each case warming one, being fastest in daily minimum temperatures.

Fig. 3 can be placed approximately here

Spatial temperature variation depended on the weather and it had a distinctive seasonal pattern. In winter, negative correlation coefficients indicate that spatial temperature differences were largest when the weather was colder than average, whereas in summer-half of the year, the largest spatial temperature differences occurred when the weather was warmer than average. The dichotomy was clear especially in average temperatures and daily maximum temperatures (Fig. 4).

Fig. 4 can be placed approximately here

4.2 Spatio-temporal variation of site-specific warmness order

The site-specific warmness order variation has seasonal differences. In case of average temperatures, daily minimum temperatures and daily maximum temperatures, the site-specific warmness order variation is largest in February. In average and daily minimum temperatures, the variation is smallest in June, and in daily maximum temperatures in May (Fig. 5).

Fig. 5 can be placed approximately here

The warmness order based rank variation has also spatial differences. In average and daily minimum temperatures, the month-specific warmness order based rank variation is most often largest in observation sites of sea prone Ruissalo island (Table 2 and Fig. 6). Occasionally also observation sites that are located more inland in relatively high positions have the largest variation. This happens in average temperatures in May, July and October and in daily minimum temperatures in February, October and December. In daily maximum temperatures, sites in Ruissalo island have largest variation in winter, site in relatively high position in spring and rural inland site Niuskala in summer and autumn.

Fig. 6 can be placed approximately here

4.3 Warmness order variation in relation to environmental factors

The relation between the unchangeable physical factors, namely topography and water bodies, and the warmness order variation of the observation sites was studied with buffer and correlation analyses. The results indicated that the water bodies were more related with the warmness order variation of the observation sites than did the topography. Of the tested buffer sizes, the correlation was strongest with the variable reflecting proportion of water bodies inside a 2 km radius buffer around the observation site (Table 3). The positive correlation coefficient indicates larger rank

variation of the observation sites in the vicinity of water bodies, whereas negative correlation coefficient indicates smaller rank variation near the water bodies. The largest positive correlation coefficients occurred for average and daily maximum temperature in February, and for daily minimum temperatures in March. The largest negative correlation coefficient occurred for daily maximum temperature in May. In case of average and daily minimum temperature, the correlation coefficient is always positive.

4.4 Spatio-temporal patterns of relative cooling and warming trends and UHI

Warmness order based ranks had statistically significant relative cooling or warming trends during majority of the months (Table 4). Significant trends were most seldom in winter, indicating that the generally larger variation observed at that season was more fluctuating and weather dependent than the variation in summer.

In average temperatures, statistically significant relative warming trend occurred most often, during 6 months out of 12, in altogether 5 observation sites (Table 5). Two of the observation sites are in the grid plan area in the city centre, two at the suburban area next to the grid plan area, and one at the south-eastern coast of Ruissalo island (see Fig. 7 and the respective figure caption). Relative cooling trend was most common in the observation site between St Michael's Church and Puistokatu street (Table 5 and Fig. 8, site 17). In daily minimum temperatures, relative warming trend occurred most often in Impivaara (Table 5 and Fig. 8, site 19), and relative cooling trend in Runosmäki and Saarnitie (Table 5 and Fig. 8, sites 26 and 30, respectively). In daily maximum temperatures, relative warming trend was most common (8/12) in Virastotalo (Table 5 and Fig. 8, site 23), and relative cooling trend in Niuskala and Rieskalähde (7/12) (Table 5 and Fig. 8, sites 49 and 20, respectively). Considering each of the calculated temperature quantities, relative warming trend was detected most often in Virastotalo and relative cooling trend in the observation site between St Michael's Church and Puistokatu street.

Regarding the five sites with most relative warming trends, new blocks of flats have been built in the surroundings of suburban sites Kupittaa and Kähäri (Fig. 8, sites 36 and 16, respectively). Sites on the southeastern coast of Ruissalo island (Fig. 8, site 9) and in the city centre on the southeastern side of the River Aura (Fig. 8, site 23) are affected by the sea and river nearby. Site 25 (Fig. 8) is located in the north-western side of the market place, where environmental changes during the study period have been rather minor. In case of market place, the positive trend practically means that in the beginning of the study period 2002-2018 the market place tended to be the second warmest after the other observation site in the city centre 300 m to the WSW of it, whereas towards the end of the study period, the market place was the warmest.

Of the five sites with most relative cooling trends, site 17 (Fig. 8) is in an urban grid plan area and sites 20, 26 and 30 (Fig. 8) are on the suburban areas where the surroundings of the observation sites have been practically unchangeable during the study period. In observation site 20, the thermometer has been shifted 8 meters southwards due to removal of lamppost in May 2013. The new site is closer to the trees in the surroundings. The high amount of months with relative cooling trends may in that case be explained with a minor microclimatic change in the form of higher evapotranspiration on the new site, especially when the majority of cooling trends exist in summer months. Fifth of the sites with relative cooling trends (Fig. 8, site 7) is in an unchangeable environment in the forest in the middle of Ruissalo island. Distance to the nearest seashore in NE is approximately 500 meters.

Fig. 7 can be placed approximately here

Fig. 8 can be placed approximately here

Of the statistically significant relative warming trends in monthly average temperature, the slope of the regression line reflecting the magnitude of change in ranks was most often, in four months, steepest in southeastern coast of Ruissalo island (Table 6 and Fig. 8, site 9) and in suburban park in Kupittaa (Fig, 8, site 36). In Ruissalo, the months with steepest slope were February, March, April and August and in Kupittaa May, October, November and December. Of the statistically significant relative cooling trends the slope of the regression line was steepest in a slightly shifted site 20 discussed above. After that, the steepest slope existed twice (Feb, Mar) in the suburban site 26 and twice (Sep, Dec) in the forested site 7 (Fig. 8).

To estimate the changes in UHI intensity during the study period, linear trend was calculated for monthly differences of average temperature between the relatively unchangeable places in the city centre and semi-urban area 3.3 km to the southeast of it (Fig. 8, sites 25 and 35, respectively). Statistically significant ($p < 0.01$) intensifying trend of UHI at a rate of 0.11°C per decade was observed (Fig. 9).

Fig. 9 can be placed approximately here

5. DISCUSSION

The global climate change has spatially variable manifestations. The results of this study indicate that variation is detectable even on an inner-city scale, and the variation has diurnal and seasonal dimensions. During the 17 year study period the variation in weather, especially the severity of winter and resulting sea ice characteristics caused largest inter-annual differences in warmness order based ranks of the observation sites. Generally, the spatial temperature differences were largest during the extreme temperature conditions - in summer during the heatwaves and in winter

during the exceptionally cold weather, the phenomenon that has been detected also in earlier studies (Hinkel et al. 2003, Wang et al. 2017).

In addition to the rather random and fluctuating weather-induced variation, relative warming or cooling trends of certain observation sites, often induced by environmental change in the neighborhood, were also observed. As during the study period, the overall trend in the study area was warming one, relative cooling can in this context in absolute terms imply either absolute cooling of the site or slower warming of the site in relation to other observation sites. Apart from the impact of environmental change, part of the observed trends were, however, strengthened, or at some sites for the most part even caused, by the frequency of weather types that favor relative warmness of certain observation sites in relation to others; the winter time North Atlantic Oscillation (NAO) Index had positive trend during the study period indicating larger proportion of mild marine south-westerly weather types towards the end of the period, the fact that largely explains the observed relative warming trends especially in the sea prone Ruissalo island, where environmental changes are negligible (NOAA 2019). The progress of climate change also has its role on the relative warming/cooling trends via its regionally varying manifestations. Similarly to the impact of increasing trend of NAO and related mildening of winters, progress of climate change has reduced and will reduce the area and thickness of winter time sea ice, and as a consequence the winter and early spring time warming effect of ice-free sea is detectable most clearly in the observation sites near the coast. The River Aura flows through the city centre, and as a result of climate change, the observed long-term trend of shortening ice cover period in winter is forecast to continue. The trend for its part supports the absolute and relative warming of the areas alongside the river in the grid plan area and further upstream (Norrgård & Helama 2019).

In general, relative cooling trends were most common in semi-urban and urban areas with rather unchangeable environment, whereas relative warming trends occurred mostly in semi-urban sites with remarkable construction works and related increased heat flux and heat storage capacity nearby (Fig. 10). Urbanisation has been considered a significant factor behind relative warming trends in other cities also (cf. Levermore et al. 2015, Luo & Lau 2019, see also Fig. 10). The impact of environmental change can also be a cooling one. Daily maximum temperatures, also strongly affected by the annual variation of sea ice, have a secondary peak in site-specific warmness order variation towards the end of the summer, the phenomenon that is explained with changes in vegetation, especially with a growth of broadleaved trees. For example in rural site Niuskala (Fig. 8, site 49, Fig. 11), approximately 10 km to the northeast of the Turku city center, the meadow on the southern side of the observation site has grown to the deciduous tree forest, resulting in remarkable change of radiation conditions in the area and as a consequence, to a relative daytime cooling in the surroundings of the observation site. The cooling impact of vegetation is discussed especially in the context of urban areas, where it is widely used as a measure to mitigate the urban heat island, especially in lower latitudes (cf. Crum et al. 2017, Kim et al. 2018).

Fig. 10 can be placed approximately here

Fig. 11 can be placed approximately here

The forecasts on the future trend of UHI intensity have not been unanimous; e.g. Wilby (2003) has predicted the strengthening of UHI, whereas Oleson et al. (2011) conclude that UHI will slightly weaken towards the forthcoming decades. In our study area, a weak (0.11 °C/decade) strengthening trend of monthly UHI intensity was observed during the study period. 17 years is, however, too short time to reliably estimate, which are relative roles of climate change, environmental change and weather, or some potential other factor(s) in the observed trend. As the immediate

neighbourhoods of the observation sites used in the UHI intensity calculations had kept unchangeable, the trend is not explained by the local environmental changes. Seasonal differences in UHI trends are also probable, and predictions on the development of fundamental factors behind the UHI suggest that the wintertime UHI will weaken in the future, if the city size keeps approximately unchangeable. As a consequence of climate change, especially winters will come warmer, and the difference between indoor and outdoor temperature will diminish resulting to a smaller thermal impact of heat leakages from buildings and heat production processes (Hinkel et al. 2003, 2007). Energy efficiency of buildings will probably also be further improved resulting in weaker winter UHI. Further development of traffic flows will have city-specific differences, but in many countries combustion engine cars will be gradually replaced by electric cars that will release less heat to the atmosphere. This could weaken the UHI at least in cities with intense traffic flow and relatively steep spatial gradient between the city centre and rural surroundings (Li et al. 2015, Kolbe 2019).

Climate change increases the probability of extreme weather conditions. Especially the heat waves will become more common in the future (Seneviratne et al. 2012). Already in the past, the heat waves have increased mortality and caused health problems at our latitudes (Näyhä 2007, Russo et al. 2015, Ruuhela et al. 2017). As our study shows the largest spatial temperature differences during the extreme temperature conditions, in addition to the risk caused by higher temperature as such, also the spatial differences in heat-related exposure will become more relevant. This study indicates that in our study area the environmental changes have mostly been warming ones and have thus strengthened the impact of climate change. The observed strengthening trend in UHI intensity can be considered a city scale indicator of unfavorable urban development from the viewpoint of climate change adaptation (cf. Cao et al. 2018).

The information on spatio-temporal temperature variation has many potential applications in urban planning, including estimation of spatial differences in cooling/heating demand, slippery conditions, thermal comfort and growing season (Chapman et al. 2001, Waffle et al. 2017, Frayssinet et al. 2018). In low latitudes, strategies to mitigate UHI are increasingly applied (Akbari & Kolokotsa 2016). Along with our observations on mostly unfavorable impacts of environmental changes on local manifestations of climate change, large site-specific fluctuation in relative warmness/coldness order observed indicates that in addition to the city scale global climate change adaptation and mitigation strategies already applied, also the climate change, weather, urban growth and land used induced local changes and variability in inner-city climate should be incorporated in urban planning with an increasing emphasis. Regular monitoring and updating, when appropriate, are also recommended.

As a consequence of global and regional climate change, climatically optimal habitats for animal and plant species can shift long distances to totally new areas, the fact that should also be recognized in spatial planning and in planning of nature conservation areas, especially (e.g. Dockerty et al. 2003, Liang et al. 2018). In our study area, the largest seasonal oscillation in relative warmness rank existed in Ruissalo island that is for the most part nature reserve (Turku 2020b). Both absolute and relative warming and cooling trends as well as large climatic variability in general are relevant ecological factors, and based on our results, we recommend the potential spatial heterogeneity in the manifestation of climate change to be sufficiently incorporated into ecological planning as well. Regarding temperature monitoring in general, the spatio-temporal dynamics of UHI observed in this study recommends the establishment of spatially dense observation network that covers sites on the broad continuum in land use / land cover, topography and coastal-inland dimension.

6. CONCLUSIONS

We studied temporal evolvement of spatial temperature differences during the 17 year (2002-2018) period in the high-latitude middle-sized coastal city of Turku, SW Finland. Based on the results, we made following key conclusions:

- Evolvement of spatial temperature differences in the study area was manifested in irregular variation and long-term relative warming and cooling trends of certain areas.
- The irregular variation was mostly related to the variation in weather, whereas relative cooling and warming trends depended mostly on land cover changes in the area.
- The strongest factor behind the irregular variation was severity of winter and related sea ice extent and thickness in the archipelago to the SW of the city.
- Relative cooling trends were most common in urban or semi-urban sites where land cover changes were negligible or nonexistent. Relative cooling of daytime temperatures was also detected as a consequence of forest growth and related micro-climatological change.
- Relative warming trends were most common in semi-urban sites where building of new blocks of flats took place in the neighbourhood during the study period, resulting in a larger anthropogenic heat release and heat storage capacity of these areas. Relative warming trends were observed also in unchangeable coastal areas as a result of more frequent south-westerly mild winter weather type towards the end of the study period.
- The UHI intensity had a weak (0.11 °C / decade) intensifying trend during the study period

As concluding remarks we stress the changing and dynamic character of UHI and spatial temperature differences in general, and recommend the intra-urban differences to be more widely incorporated in climate-related urban planning. We also encourage to monitor and update the plans regularly.

Acknowledgements

Financial support in the form of personal scholarship (JS) for this research was provided by the Urban Research Program of the city of Turku. Financial support for the weather observation equipment has been provided by the Geography Section of the University of Turku and by the Urban Environment Division of the City of Turku.

References

Akbari K, Kolokotsa D (2016) Three decades of urban heat islands and mitigation technologies research. Energ Buildings 133:834–842

Cao Q, Yu D, Georgescu M, Wu J, Wang W (2018) Impacts of future urban expansion on summer climate and heat-related human health in eastern China. Environment International 112:134–146

Chapman L, Thornes JE, Bradley AV (2001) Modeling of road surface temperatures from a geographical parameter database. Part 1, statistical. Meteorol Appl 8:409–419

Cleugh HA, Oke TR (1986) Suburban-rural energy balance comparisons in summer for Vancouver, B.C. Bound-Lay Meteorol 36:351–369

Cotton WR, Pielke RA (1995) Human impacts on weather and climate. Cambridge University Press, Cambridge

Crum SM, Shiflett SA, Jenerette GD (2017) The influence of vegetation, mesoclimate and meteorology on urban atmospheric microclimates across a coastal to desert climate gradient. J Environ Manage 200:295–303

Dockerty T, Lovett A, Watkinson A (2003) Climate change and nature reserves: examining the potential impacts, with examples from Great Britain. Global Environ Chang 13:125–135

Emmanuel R, Krüger E (2012) Urban heat island and its impact on climate change resilience in a shrinking city: The case of Glasgow, UK. Build Environ 53:137–149

Estoque RC, Murayama Y (2017) Monitoring surface urban heat island formation in a tropical mountain city using Landsat data (1987–2015). ISPRS J Photogramm 133:18–29

FMI (2019) Climateguide.fi. Finnish Meteorological Institute. https://ilmasto-opas.fi/en (accessed 27 March 2019)

FMI (2020) Itämeren jäätalvet (Ice conditions in Baltic Sea during the winters). Finnish Meteorological Institute. https://www.ilmatieteenlaitos.fi/jaatalvet (accessed 22 May 2020)

Frayssinet L, Merlier L, Kuznik F, Hubert J-L., Milliez M, Roux J.-J (2018) Modeling the heating and cooling energy demand of urban buildings at city scale. Renew Sust Energ Rev 81:2318–2327

Grimmond CSB, Roth M, Oke TR, Au YC, Best M, Betts R, Carmichael G, Cleugh H, Dabberdt W, Emmanuel R, Freitas E (2010) Climate and More Sustainable Cities: Climate Information for Improved Planning and Management of Cities (Producers/Capabilities Perspective). Procedia Environ Sci 1:247–274

Hinkel KM, Nelson FE, Klene AE, Bell JH (2003) The urban heat island in winter at Barrow, Alaska. Int J Climatol 23:1889–1905

Hinkel KM, Nelson FE (2007) Anthropogenic heat island at Barrow, Alaska, during winter: 2001–2005. J Geophys Res-Atmos 112:D06118

Hjort J, Suomi J, Käyhkö J (2016) Extreme urban–rural temperatures in the coastal city of Turku, Finland: Quantification and visualization based on a generalized additive model. Sci Total Environ 569–570:507–517

Huovila S (1987) Pienilmasto (Microclimate). In: Alalammi P (ed) Atlas of Finland 131. Maanmittaushallitus, Helsinki, p 23–26

Kim H, Gu D, Kim HY (2018) Effects of Urban Heat Island mitigation in various climate zones in the United States. Sustain Cities Soc 41:841–852

Klysik K (1996) Spatial and seasonal distribution of anthropogenic heat emissions in Lodz, Poland. Atmos Environ 30:3397–3404

Kolbe K (2019) Mitigating urban heat island effect and carbon dioxide emissions through different mobility concepts: Comparison of conventional vehicles with electric vehicles, hydrogen vehicles and public transportation. Transp Policy 80:1–11

Kolokotroni M, Giridharan R (2008) Urban heat island intensity in London: an investigation of the impact of physical characteristics on changes in outdoor air temperature during summer. Sol Energy 82:986–998

Landsberg HE (1981) The Urban Climate. Academic Press, London

Levermore GJ, Parkinson JB, Laycock PJ, Lindley S (2015) The Urban Heat Island in Manchester 1996-2011. Build Serv Eng Res T 36(3):343–356

Levermore G, Parkinson J, Lee K, Laycock P, Lindley S (2018) The increasing trend of the urban heat island intensity. Urban Clim 24:360–368

Li C, Cao Y, Zhang M, Wang J, Liu J, Shi H, Geng Y (2015) Hidden Benefits of Electric Vehicles for Addressing Climate Change. Sci Rep 5:9213

Liang J, Xing W, Guangming Z, Li X, Peng Y, Li X, Gao X, He X (2018) Where will threatened migratory birds go under climate change? Implications for China's national nature reserves. Sci Total Environ 645:1040–1047

Liu W, Ji C, Zhong J, Jiang X, Zheng Z (2007) Temporal characteristics of the Beijing urban heat island. Theor Appl Climatol 87:213–221

Liu L, Lin Y, Liu J, Wang L, Wang D, Shui T, Chen X, Wu Q (2017) Analysis of local-scale urban heat island characteristics using an integrated method of mobile measurement and GIS-based spatial interpolation. Build Environ 117:191–207

Luo M, Lau N (2019) Characteristics of summer heat stress in China during 1979–2014: climatology and long-term trends. Clim Dyn 53:5375–5388

Magee N, Curtis J, Wendler G (1999) The urban heat island effect at Fairbanks, Alaska. Theor Appl Climatol 64:39–47

Nichol J, Hang TP, Ng E (2014) Temperature projection in a tropical city using remote sensing and dynamic modeling. Clim Dyn 42:2921–2929

NLS (2000) Elevation model 2000, 25 m x 25 m, TIFF. National Land Survey of Finland. CSC - IT Center for Science Ltd, 2015-10-08T00:00:00-00:00, urn:nbn:fi:csc-kata00001000000000000319 (Accessed 22 Oct 2019)

NLS (2010) SLICES 2010, 10 m x 10 m, generalized raster, ETRS-TM35FIN. National Land Survey of Finland. CSC - IT Center for Science Ltd, 2015-10-14T00:00:00-00:00, urn:nbn:fi:csc-kata00001000000000000262 (accessed 22 May 2020)

NOAA (2019) Monthly mean NAO index since January 1950. National Oceanic and Atmospheric Administration. National Weather Service. Climate Prediction Center. https://www.cpc.ncep.noaa.gov/products/precip/CWlink/pna/nao_index.html (accessed 18 Nov 2019)

Norrgård S, Helama S (2019) Historical trends in spring ice breakup for the Aura River in Southwest Finland, AD 1749–2018. The Holocene 29(6):953–963

Näyhä S (2007) Heat mortality in Finland in the 2000s. Int J Circumpol Heal 66:418–424

Oke TR (1973) City size and the urban heat island. Atmos Environ 7:769–779

Oke TR (1981) Canyon geometry and the nocturnal urban heat island: Comparison of scale model and field observations. Int J Climatol 1:237–254

Oke TR (1987) Boundary Layer Climates. 2nd edition. Routledge, London

Oleson KW, Bonan GB, Feddema J, Jackson T (2011) An examination of urban heat island characteristics in a global climate model. Int J Climatol 31:1848–1865

Peel MC, Finlayson BM, McMahon TA (2007) Updated world map of the Köppen-Geiger climate classification. Hydrol Earth Syst Sc 11:1633–1644

Pirinen P, Simola S, Aalto J, Kaukoranta J-P, Karlsson P, Ruuhela R (2012) Tilastoja Suomen ilmastosta 1981–2010 (Climatological statistics of Finland 1981–2010). Raportteja 2012: 1. http://hdl.handle.net/10138/35880 (accessed 18 Sep 2019)

Russo S, Sillmann J, Fischer EF (2015) Top ten European heatwaves since 1950 and their occurrence in the coming decades. Environ Res Lett 10:1–15

Ruuhela R, Jylhä K, Lanki T, Tiittanen P, Matzarakis A (2017) Biometeorological Assessment of Mortality Related to Extreme Temperatures in Helsinki Region, Finland, 1972–2014. Int J Env Res Pub He 14(8):944

Schwarz N, Schlink U, Franck U, Grossmann K (2012) Relationship of land surface and air temperatures and its implications for quantifying urban heat island indicators – an application for the city of Leipzig (Germany). Ecol Indic 18:693–704

Seinä A, Peltola J (1991) Duration of the ice season and statistics of fast ice thickness along the Finnish coast 1961-1990. Finnish Marine Research N:o 258. http://hdl.handle.net/10138/167792 (accessed 24 Nov 2019)

Seinä A, Eriksson P, Kalliosaari S, Vainio J (2006) Ice seasons 2001-2005 in Finnish sea areas. Report Series of the Finnish Institute of Marine Research 57. http://hdl.handle.net/10138/157956 (accessed 24 Nov 2019)

Seneviratne SI, Nicholls N, Easterling D, Goodess CM, Kanae S, Kossin J, Luo Y, Marengo J, McInnes K, Rahimi M, Reichstein M, Sorteberg A. Vera C, Zhang X (2012) Changes in climate extremes and their impacts on the natura lphysical environment. In: Field CB, Barros V, Stocker TF, Qin D, Dokken DJ, Ebi KL, Mastrandrea MD, Mach KJ, Plattner G-K, Allen SK, Tignor M, Midgley PM (eds) Managing the Risks of Extreme Events and Disasters to Advance Climate Change Adaptation. A Special Report of Working Groups I and II of the Intergovernmental Panel on Climate Change (IPCC). Cambridge University Press, Cambridge, UK, and New York, NY, USA, p 109–230

Sillmann J, Thorarinsdottir T, Keenlyside N, Schaller N, Alexander LV, Hegerl G, Seneviratne SI, Vautard R, Zhang X, Zwiers FW (2017) Understanding, modeling and predicting weather and climate extremes: Challenges and opportunities. Weather Clim Extrem 18:65–74

Suomi J (2014) Characteristics of urban heat island (UHI) in a high-latitude coastal city - a case study of Turku, SW Finland. PhD dissertation. University of Turku, Finland.

Suomi J (2018) Extreme temperature differences in the city of Lahti, southern Finland: Intensity, seasonality and environmental drivers. Weather Clim Extremes 19:20–28

Suomi J, Hjort J, Käyhkö J (2012) Effects of scale on modelling the urban heat island in Turku, SW Finland. Clim Res 55:121–136

Suomi J, Käyhkö J (2012) The impact of environmental factors on urban temperature variability in the coastal city of Turku, SW Finland. Int J Climatol 32:451–463

SYKE (2019) Producing land cover and land use data in CORINE Land Cover 2018 project and validating Copernicus Land products in Finland. Suomen Ympäristökeskus – Finnish Environment Institute. https://www.syke.fi/en-US/Research__Development/Research_and_development_projects/Projects/Producing_land_cover_and_land_use_data_in_CORINE_Land_Cover_2018_project_in_Finland (accessed 28 Apr 2020)

Szymanowski M, Kryza M (2009) GIS-based techniques for urban heat island spatialization. Clim Res 38:171–187

Turku (2020a) Turku map service. City of Turku. https://opaskartta.turku.fi (accessed 14 Aug 2020)

Turku (2020b) Nature Reserves: Ruissalo. City of Turku. https://www.turku.fi/en/culture-and-sports/recreation/nature-reserves/ruissalo (accessed 7 Feb 2020)

UN (2018) 68% of the world population projected to live in urban areas by 2050, says UN. United Nations. Department of Economic and Social Affairs. https://www.un.org/development/desa/en/news/population/2018-revision-of-world-urbanization-prospects.html (accessed 8 Oct 2020)

Väyrynen R, Suomi J, Käyhkö J (2017) Fine-scale analysis of sea effect on coastal air temperatures at different time scales. Boreal Environ Res 22:369–383

Waffle AD, Corry RC, Gillespie TJ, Brown RD (2017) Urban heat islands as agricultural opportunities: An innovative approach. Landscape Urban Plan 161:103–114

Wang C, Myint SW, Wang Z, Song J (2016) Spatio-temporal modeling of the urban heat island in the Phoenix metropolitan area: Land use change implications. Remote Sensing, 8(3):185

Wang J, Yan Z, Quan X, Feng J (2017) Urban warming in the 2013 summer heat wave in eastern China. Clim Dyn 48:3015–3033

Wienert U, Kuttler W (2005) The dependence of the urban heat island intensity on latitude – A statistical approach. Meteorol Z 14(5):677–686

Wilby (2003) Past and projected trends in London's urban heat island. Weather 58:251–260

Yao R, Wang L, Huang X, Niu Z, Liu F, Wang Q (2017) Temporal trends of surface urban heat islands and associated determinants in major Chinese cities. Sci Total Environ 609:742–754

Zhang H, Qi Z, Ye X, Cai Y, Ma W, Chen M (2013) Analysis of land use/land cover change, population shift, and their effects on spatiotemporal patterns of urban heat islands in metropolitan Shanghai, China. Appl Geogr 44:121–133

Zhou D, Zhao S, Liu S, Zhang L, Zhu C (2014) Surface urban heat island in China's 32 major cities: Spatial patterns and drivers. Remote Sens Environ 152:51–61

Zhou D, Zhang L, Hao L, Sun G, Liu Y, Zhu C (2016) Spatiotemporal trends of urban heat island effect along the urban development intensity gradient in China. Sci Total Environ 544:617–626

Tables and respective table captions

Table 1. Characteristics of the observation sites. Land use / land cover refers to the most common land use /land cover form inside 100 m radius buffer around the observation site, determined by the SLICES 2010 land use classification (NLS 2010). The site numbers corresponds with the numbers in Figs 6 and 8

Site number	Regional characteristic	Land use / land cover in the surroundings	Elevation (m.a.s.l.)
1	Rural	Water	0.5
2	Rural	Grass	1.5
3	Semi-urban	Forest	4.4
4	Rural	Forest	0.5
5	Rural	Forest	36.3
6	Semi-urban	Forest	10.1
7	Rural	Forest	17.3
8	Rural	Grass	4.6
9	Rural	Field	1.0
10	Semi-urban	Road/street	6.0
11	Rural	Forest	0.8
12	Semi-urban	Gravel	2.5
13	Semi-urban	Forest	22.2
14	Urban	Road/street	2.3
15	Rural	Forest	22.5
16	Semi-urban	Detached houses	20.9
17	Urban	Road/street	9.8
18	Urban	Railway	9.7
19	Semi-urban	Road/street	26.2
20	Semi-urban	Forest	32.3
21	Semi-urban	Park	23.5
22	Urban	Blocks of flats	16.9
23	Urban	Road/street	7.2
24	Semi-urban	Park	28.9
25	Urban	Road/street	7.7
26	Urban	Blocks of flats	37.6
27	Urban	Blocks of flats	33.5
28	Rural	Meadow	6.5
29	Rural	Forest	43.5
30	Semi-urban	Detached houses	16.8
31	Semi-urban	Row houses	9.7
32	Semi-urban	Blocks of flats	21.0
33	Urban	Blocks of flats	22.0
34	Urban	Blocks of flats	23.2
35	Semi-urban	Forest	13.8
36	Semi-urban	Park	17.3
37	Semi-urban	Detached houses	15.2
38	Semi-urban	Detached houses	21.6
39	Rural	Forest	24.9

40	Semi-urban	Detached houses	29.9
41	Semi-urban	Detached houses	22.7
42	Rural	Field	18.8
43	Semi-urban	Forest	15.2
44	Semi-urban	Blocks of flats	47.7
45	Rural	Field	13.5
46	Rural	Field	33.8
47	Rural	Field	21.3
48	Semi-urban	Blocks of flats	56.6
49	Rural	Forest	32.4
50	Semi-urban	Detached houses	17.3
51	Semi-urban	Detached houses	39.7
52	Rural	Meadow	14.1

Table 2. Sites with largest variation in monthly warmness order based ranks in 2002-2018. The first number(s) refer(s) to the observation site number(s) in Fig. 6. The first number in parentheses tells the rank variation and the latter number the amount of observation sites included in the analyses.

Month	Average temperature	Daily minima	Daily maxima
Jan	5 (25/41)	2 (27/41)	7 (23/41)
Feb	2, 5 (32/42)	2, 44 (31/42)	2 (36/42)
Mar	1, 5 (31/42)	2 (34/42)	29 (38/42)
Apr	2, 5 (23/41)	1 (25/41)	29 (34/41)
May	44 (14/34)	2 (15/35)	49 (16/34)
Jun	3 (15/40)	9 (14/40)	49 (37/40)
Jul	20 (17/39)	9 (17/39)	49 (36/39)
Aug	5 (20/39)	9 (18/39)	49 (37/39)
Sep	5, 11 (16/35)	51 (12/35)	49 (33/35)
Oct	5, 44 (17/34)	29 (15/34)	49 (30/34)
Nov	19 (20/39)	10 (21/39)	19 (25/39)
Dec	5 (19/39)	29 (20/39)	19 (30/40)

Table 3. Correlation coefficients between the site-specific warmness order based rank variation (range length between highest and lowest rank) and water cover inside the 2 km radius buffer around the observation site

Month	Average	Daily min	Daily max
Jan	0.393*	0.389*	0.406**
Feb	0.581**	0.435**	0.588**
Mar	0.549**	0.576**	0.211
Apr	0.473**	0.495**	-0.360*
May	0.048	0.353*	-0.488**
Jun	0.462**	0.285	-0.176
Jul	0.309	0.237	-0.167
Aug	0.355*	0.306	-0.278
Sep	0.445**	0.286	-0.273
Oct	0.335	0.029	0.142

Nov	0.008	0.041	0.074
Dec	0.170	0.097	0.042

**=correlation is statistically significant at P level ≤0.01
*=correlation is statistically significant at P level ≤0.05

Table 4. Number of sites with statistically significant ($p \leq 0.05$) relative warming (+) and cooling (-) trends in 2002-2018

	Average temps		Daily minima		Daily maxima	
	+	-	+	-	+	-
Jan	4	2	1	0	4	5
Feb	3	5	1	2	4	3
Mar	3	3	1	4	3	3
Apr	6	6	5	5	4	6
May	7	4	4	2	6	4
Jun	5	6	5	4	8	5
Jul	3	4	4	3	7	4
Aug	5	6	5	4	7	5
Sep	3	2	3	2	12	6
Oct	5	3	3	1	6	6
Nov	6	5	2	1	6	5
Dec	3	6	2	5	5	6
Total	53	52	36	33	72	58

Table 5. Number of months with statistically significant ($p \leq 0.05$) relative warming (+) and cooling (-) trends for the sites with an uninterrupted observation period in 2002-2018. Number in parentheses refers to the observation site location in Fig. 8

	Average temp		Daily minima		Daily maxima		Total	
	+	-	+	-	+	-	+	-
Alfa (32)	0	2	0	0	0	3	0	5
Hautausmaa (39)	0	1	0	0	0	2	0	3
Hiiriluoto, inland (7)	0	3	0	2	0	4	0	9
Hiiriluoto, hill (5)	0	1	0	0	1	1	1	2
Hirvensalo (11)	0	1	0	1	2	2	2	4
Impivaara (19)	1	1	5	0	2	1	8	2
Kauppatori (25)	6	0	4	0	5	0	15	0
Kupittaa (36)	6	0	4	0	3	0	13	0
Kähäri (16)	6	0	1	0	6	0	13	0
Linna (14)	2	0	0	0	0	0	2	0
Messukeskus (10)	0	0	0	1	0	0	0	1
Metsämäki (47)	1	1	2	0	2	2	5	3
Mikaelinkirkko (17)	0	8	0	2	0	6	0	16
Niuskala (49)	0	0	0	0	0	7	0	7
Pansio (3)	0	0	1	1	0	1	1	2

Perno (6)	2	0	0	0	2	0	4	0
Pääskyvuori (44)	2	0	0	1	6	1	8	2
Rieskalähde (20)	0	4	0	0	0	7	0	11
Ruissalo (9)	6	0	4	0	2	0	12	0
Runosmäki (26)	0	6	0	4	0	4	0	14
Ryhmäpuutarha (35)	0	0	0	0	1	0	1	0
Saarnitie (30)	0	4	0	4	1	0	1	8
Vapaavarasto (12)	2	0	0	0	2	0	4	0
Virastotalo (23)	6	0	2	0	8	0	16	0

Table 6. Slope of the trend line reflecting statistically significant ($p \leq 0.05$) relative cooling (-) or warming (+) of the observation site's monthly average temperature during the observation period 2002-2018. For each month, the fastest warming trend is **bolded** and the fastest cooling trend is written in *italics*

Observation site	Jan	Feb	Mar	Apr	May	Jun	Jul	Aug	Sep	Oct	Nov	Dec
Alfa (32)				-0.23						*-0.23*		
Hautausmaa (39)								-0.3				
Hiiriluoto, inl. (7)						-0.25			*-0.45*			*-0.48*
Hiiriluoto, hill (5)						-0.35						
Hirvensalo (11)											*-0.37*	
Impivaara (19)				*-0.41*						0.23		
Kauppatori (25)	0.08	0.06	0.09							0.09	0.08	0.06
Kupittaa (36)				0.46	**0.29**				0.39	**0.43**	**0.43**	**0.48**
Kähäri (16)	0.37	0.49			**0.29**				**0.42**	0.31	0.32	
Linna (14)					0.11		0.23					
Messukeskus (10)												
Metsämäki (47)				-0.32		0.19						
Mikaelink. (17)	*-0.13*			-0.18	-0.15	-0.25	-0.32	-0.22			-0.12	-0.2
Niuskala (49)												
Pansio (3)					-0.31							-0.35
Perno (6)	**0.42**							0.18				
Pääskyvuori (44)						**0.28**	**0.45**					
Rieskalähde (20)					*-0.49*	*-0.62*	*-0.63*	*-0.52*				
Ruissalo (9)		**0.68**	**0.85**	**0.74**	0.22			**0.68**			0.17	
Runosmäki (26)		*-0.61*	*-0.61*	-0.4		-0.23		-0.35				-0.32
Ryhmäpuut. (35)												
Saarnitie (30)		-0.39						-0.3	-0.34		-0.30	
Vapaavarasto (12)					0.25						0.18	
Virastotalo (23)				0.14	0.18	0.13	0.25	0.27	0.20			
N	41	42	42	41	34	40	39	39	35	34	39	39

Figures and respective figure captions

Fig. 1. An example of the observation site in Kähäri, a suburban area to the north-west of the city centre

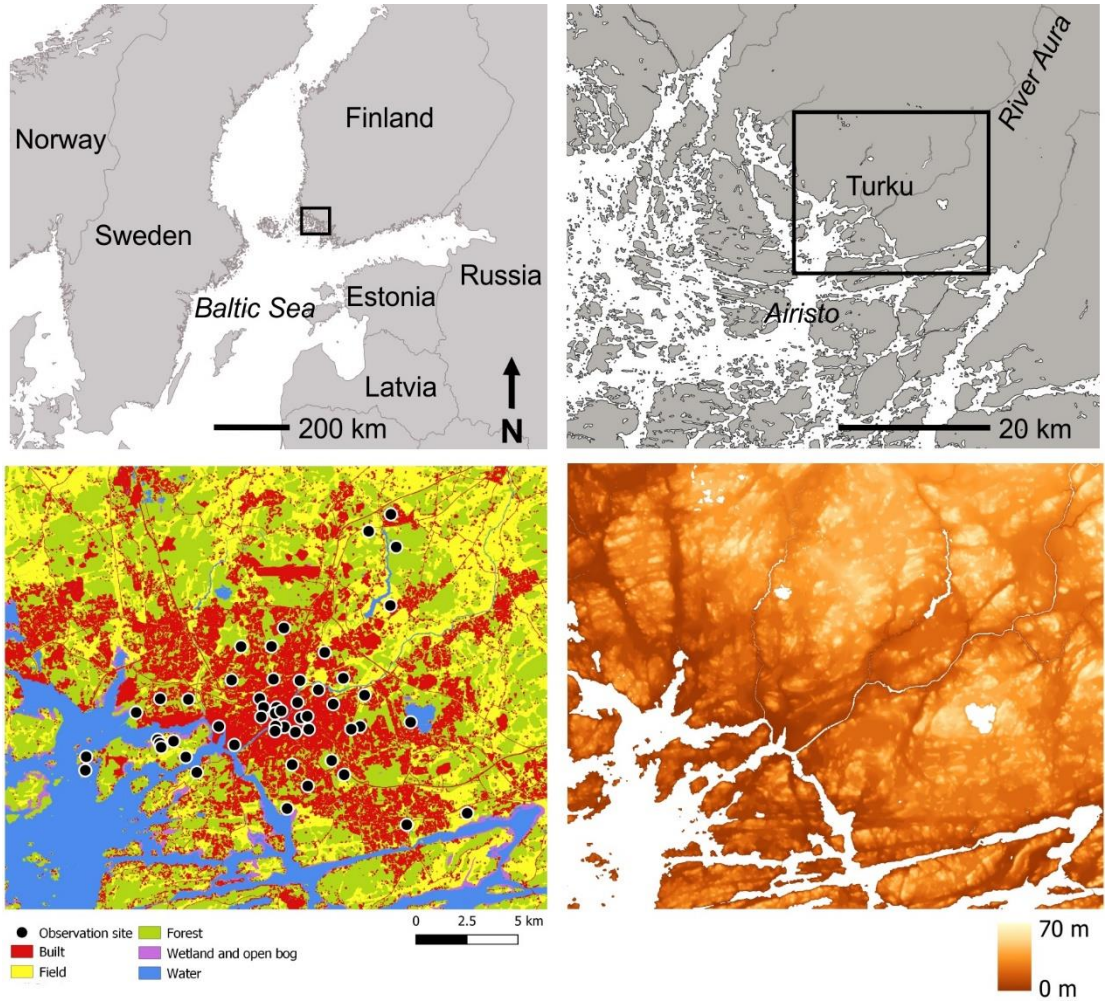

Fig. 2. The study area in the south-western Finland with principal land cover, topography (elevation above the sea level) and temperature observation sites that are involved in the analyses

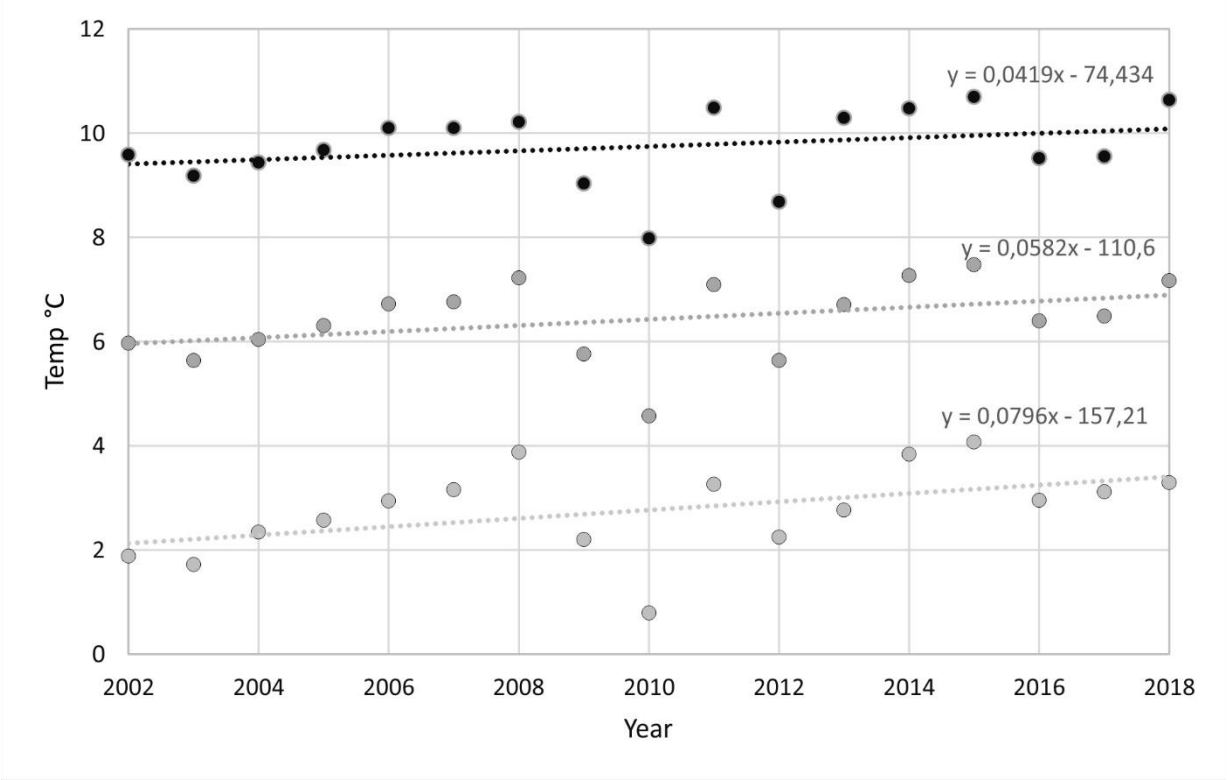

Fig. 3. Annual average temperature, annual average of daily minimum temperature and annual average of daily maximum temperature of 24 temperature loggers with uninterrupted observation period 2002-2018 with the respective trend lines and related equations

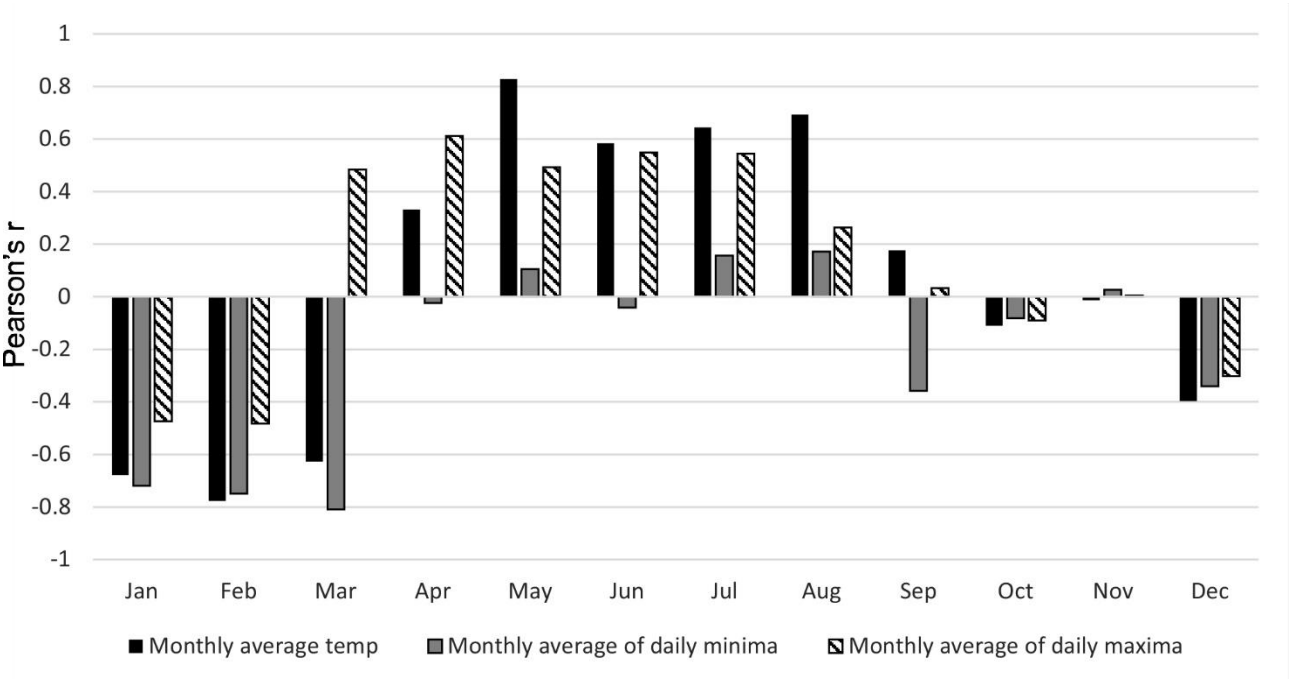

Fig. 4. Correlation coefficients between the standard deviation of the monthly average temperatures vs. temperature anomaly from the long time average (1981-2010) temperature

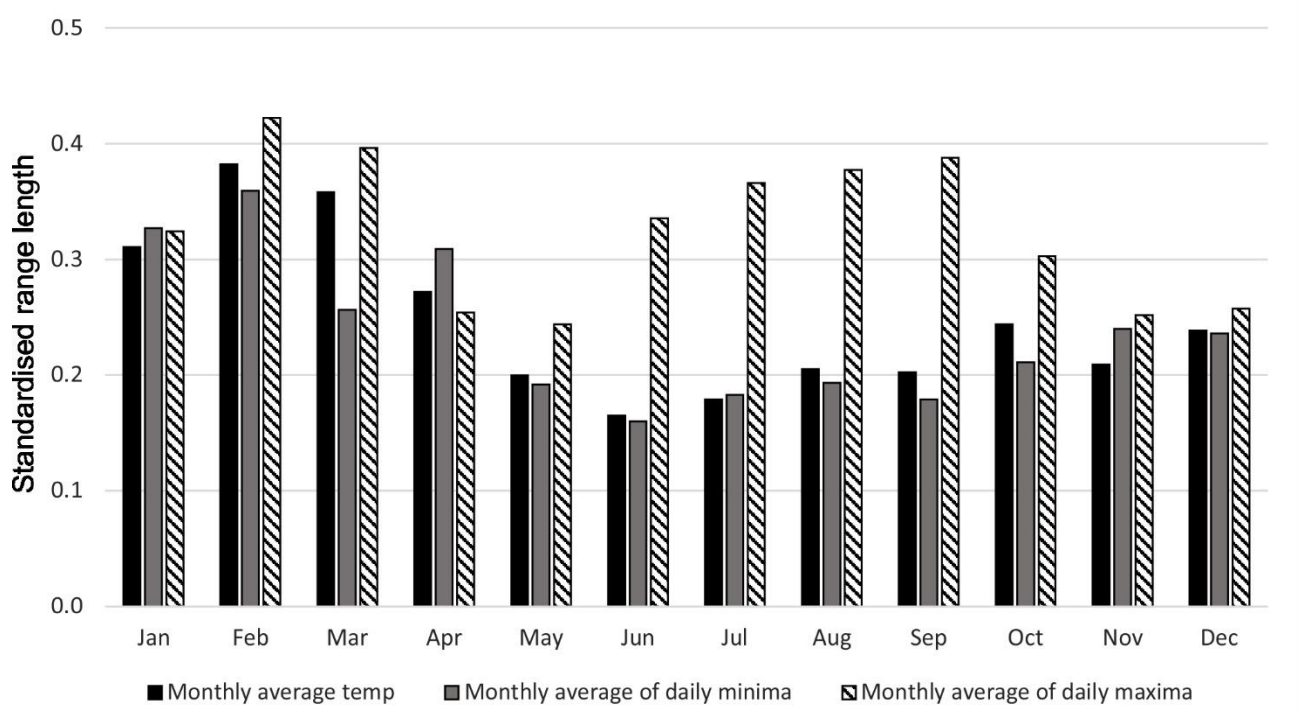

Fig. 5. Monthly standardised range lengths (highest rank – lowest rank / amount of observation sites) of warmness order based ranks during the observation period 2002-2018

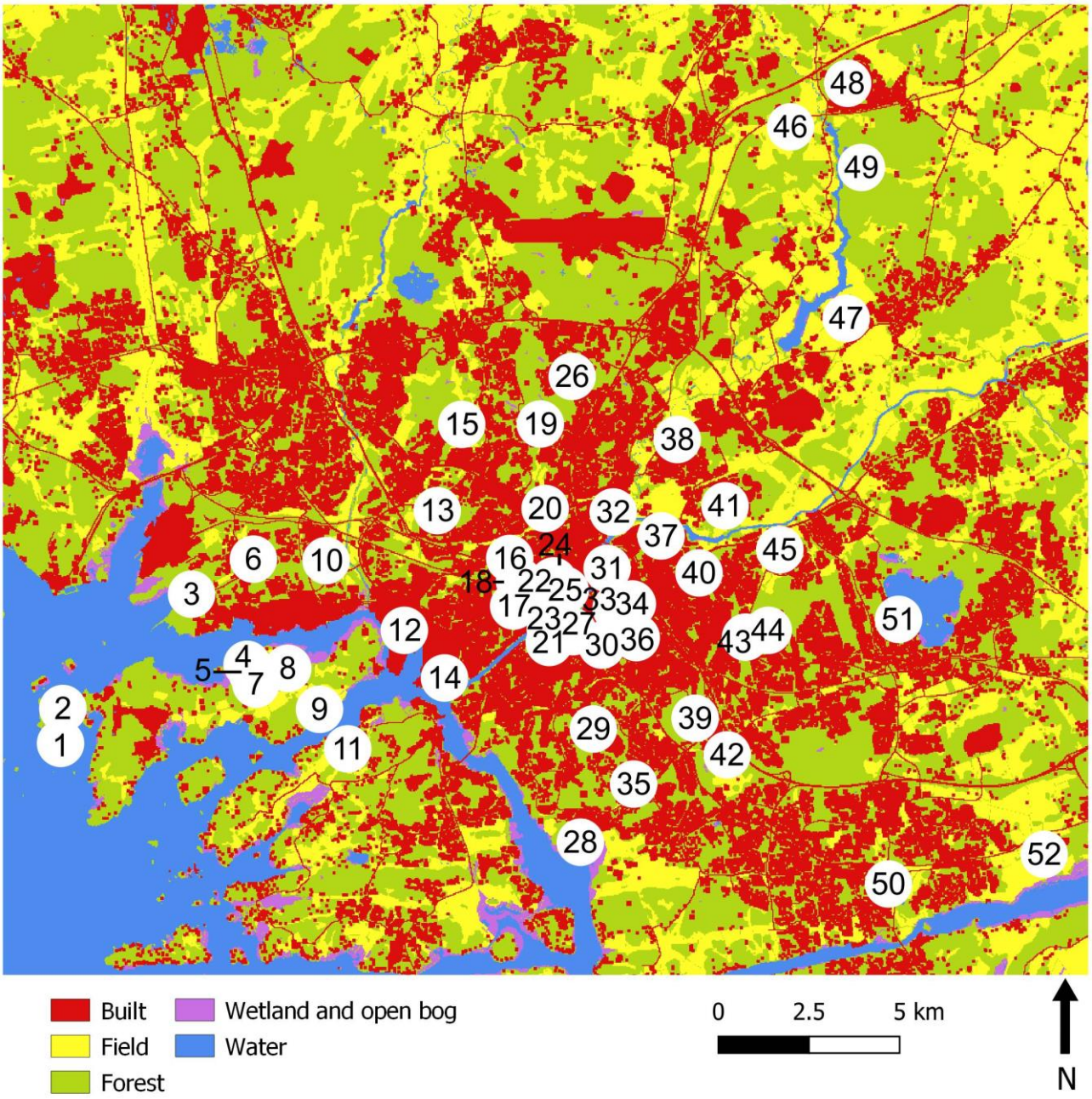

Fig. 6. Temperature observation sites numbered consecutively from west to east

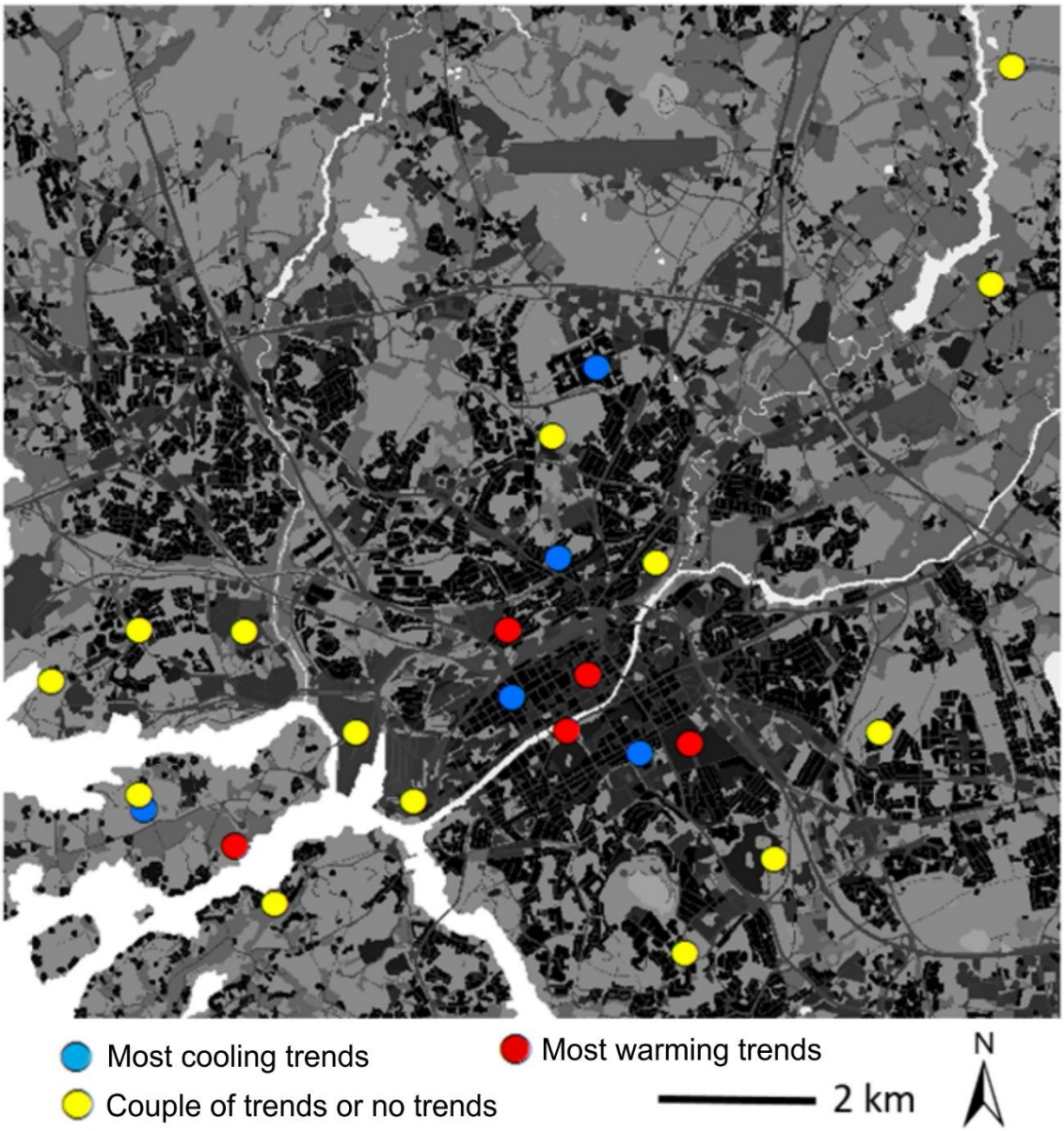

Fig. 7. The 24 temperature observation sites with uninterrupted observation period. Five sites with most relative cooling and warming trends (grandtotal of month-specific average, daily minimum and daily maximum temperatures) in 2002-2018 are identified with colour. The sites with most warming trends are the same for monthly average temperatures and for grandtotal of month-specific average, daily minimum and daily maximum temperatures

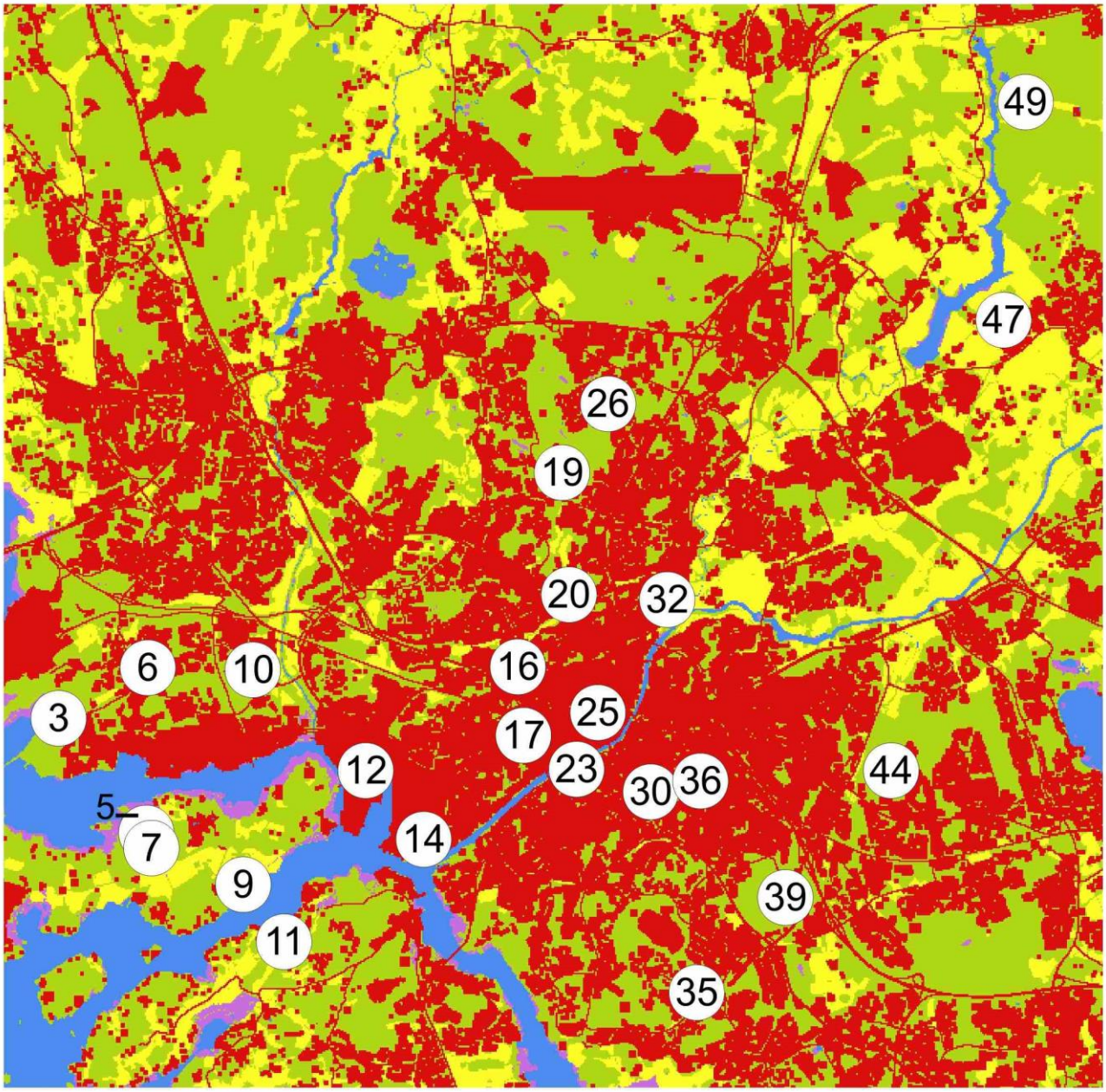

Fig. 8. The temperature observation sites with uninterrupted observation period. The observation site numbers link the sites to the site names in Tables 5 and 6

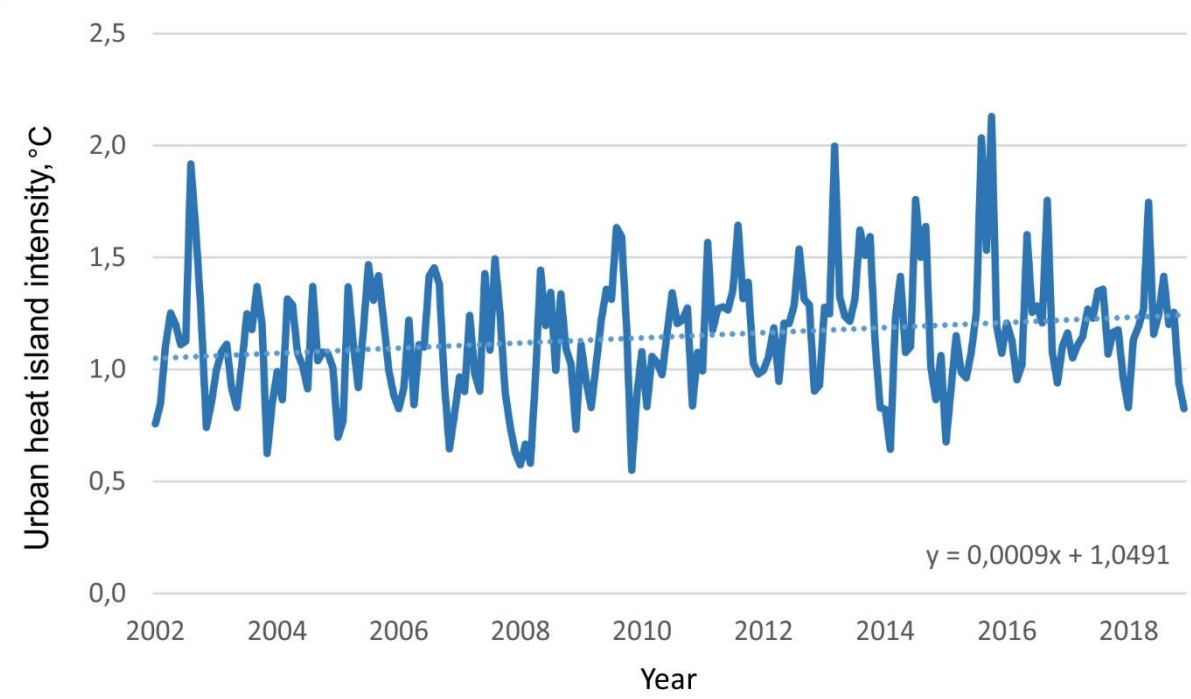

Fig. 9. Trend in UHI intensity during the study period 2002-2018

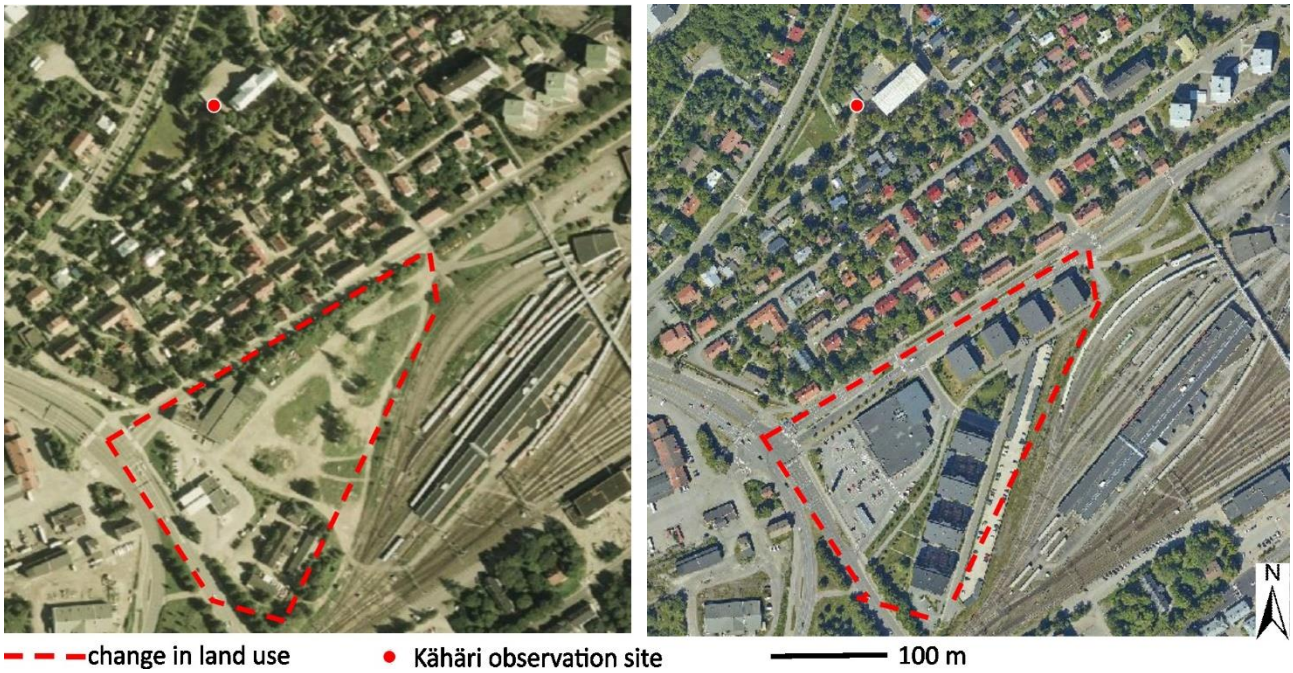

Fig. 10. Environmental change to the south of Kähäri observation site (Fig. 8, site 16) during the study period 2002-2018. Aerial photos (Turku 2020a) taken 2002 (left) and 2018 (right)

Fig. 11. Environmental change to the south of Niuskala observation site (Fig. 8, site 49) during the study period 2002-2018. Aerial photos (Turku 2020a) taken 2002 (left) and 2015 (right)